GEOLOGY | THE GEOLOGICAL SOCIETY OF AMERICA®

https://doi.org/10.1130/G49097.1

Manuscript received 10 July 2020
Revised manuscript received 27 March 2021
Manuscript accepted 30 March 2021

Published online 3 June 2021

Serpentinized peridotite versus thick mafic crust at the Romanche oceanic transform fault

Emma P.M. Gregory*, Satish C. Singh, Milena Marjanović and Zhikai Wang
Institut de Physique du Globe de Paris, Université de Paris, CNRS, 1 rue Jussieu, 75005 Paris, France

ABSTRACT

The crust beneath transform faults at slow-spreading ridges has been considered to be thin, comprising a thin mafic layer overlying serpentinized peridotite. Using wide-angle seismic data, we report the presence of a Moho at ~6 km depth and a low-velocity anomaly extending down to 9 km beneath the 20-km-wide Romanche transform valley floor in the equatorial Atlantic Ocean. The low crustal velocities above the Moho could be due to either highly serpentinized mantle peridotite or fractured mafic rocks. The existence of clear Moho reflections and the occurrence of a large crustal-depth rupture during the 2016 magnitude 7.1 earthquake suggest that the crust likely consists of fractured mafic material. Furthermore, the presence of low velocities below the Moho advocates for extensive serpentinization of the mantle, indicating that the Moho reflection is unlikely to be produced by a serpentinization front. The crust to the north of the transform fault likely consists of mafic material, but that in the south appears to be more amagmatic, possibly containing serpentinized peridotite. Our results imply that the transform fault structure is complex and highly heterogeneous, and thus would have significant influence on earthquake rupture and alteration processes.

INTRODUCTION

Oceanic transform faults (OTFs) comprise over 40% of mid-ocean-ridge (MOR) spreading systems (Bird, 2003), with their inactive traces—fracture zones (FZs)—extending across entire ocean basins. OTFs exhibit more variable topography than spreading centers (e.g., Maia et al., 2016), are capable of producing large ($M > 7$) earthquakes (McGuire et al., 1996), and are important sites for fluid circulation and alteration within the lithosphere (Hensen et al., 2019). Despite the ubiquity of OTFs, there is a lack of modern and comprehensive studies, especially when compared to spreading centers.

OTFs offsetting slow-spreading ridges are thought to exhibit thinned crust, comprising a thin mafic layer overlying serpentinized mantle rocks (Detrick et al., 1993). This perception is mainly based on the recovery of serpentinized peridotites from OTF valleys and bounding walls (Prinz et al., 1976; Cannat et al., 1991) and early geophysical studies showing an absence of a gabbroic crustal section (White et al., 1984; Whitmarsh and Calvert, 1986; Detrick et al., 1993). This is consistent with the idea that the cooling effect of the older lithosphere juxtaposed opposite spreading centers at ridge-transform intersections (RTIs) reduces melting (e.g., White et al., 1984; Bonatti et al., 2001). This effect may be enhanced in slow-spreading environments where mantle upwelling is often focused at segment centers (Blackman and Forsyth, 1989; Hooft et al., 2000). Conversely, fast-slipping OTFs in the Pacific Ocean, often with small age contrasts, are suggested to consist of normal-thickness, fractured mafic crust (Van Avendonk et al., 1998; Roland et al., 2012). We present the results of a geophysical study across the slow-slipping Romanche OTF in the Atlantic Ocean, the longest active OTF on Earth.

ROMANCHE TRANSFORM FAULT

Located in the equatorial Atlantic Ocean, the Romanche OTF offsets the Mid-Atlantic Ridge (MAR) by ~880 km (Fig. 1A), with a slip rate of ~3.2 cm/yr (DeMets et al., 2010) and a maximum lithospheric age contrast of 45 m.y. The fault is not orthogonal to the ridge axis and displays complex bathymetry, with local highs as shallow as ~900 m and deep valleys at ~7800 m, likely caused by transpressive and transtensional stresses due to the oblique geometry (Bonatti et al., 1994). To the north of the active transform, there lies an ~100-km-wide zone of ridges and valleys (Fig. 1), representing previous traces of the transform fault (TF) that were active until ca. 10–8 Ma (Bonatti et al., 1994), leading to a "multifault" transform system (Ligi et al., 2002) caused by the large offset and thermal contrast across the fault. An ~300-km-long transverse ridge rises ~4500 m from the seafloor opposite the eastern RTI, which may represent a sliver of lithosphere uplifted by transpressional stress (Bonatti et al., 1994).

Sampling expeditions (Fig. 1C) have found a widespread presence of serpentinized peridotites along the transform valley (Bonatti, 1968), the majority of which are plagioclase-bearing due to their impregnation with basaltic melt (Seyler and Bonatti, 1997). An asymmetry in petrology is observed across the fault, with basalts and gabbros to the north of the TF, and mainly serpentinized peridotites to the south (Bonatti, 1968; Bonatti and Honnorez, 1976), reflecting the differences in spreading style at the MAR. To the north, classic abyssal hill structures suggest a relatively magmatic spreading segment (Fig. 1). To the south, the northern half of the segment is oblique, stepping westward in a series of non-transform offsets and exhibiting an irregular seafloor fabric consistent with tectonically dominated spreading.

SEISMIC REFRACTION EXPERIMENT

In 2018, an 850-km-long, wide-angle seismic profile was acquired across the Romanche TF and St. Paul and Chain FZs (Marjanović et al., 2020). We focus on the part of the profile crossing the eastern Romanche TF from the 8 Ma South American plate to the 40 Ma Nubian plate, ~60 km west of the RTI. We used records from 28 ocean bottom seismographs (OBSs), spaced, on average, 14.2 km apart. Shot spacing was 300 m. To perform seismic tomographic inversion, wide-angle arrivals from the crust (Pg) and mantle (Pn), and reflections from the Moho (PmP) were identified (see Fig. S1 in the

*E-mail: epmgregory@gmail.com

CITATION: Gregory, E.P.M., et al., 2021, Serpentinized peridotite versus thick mafic crust at the Romanche oceanic transform fault: Geology, v. 49, p. 1132–1136, https://doi.org/10.1130/G49097.1

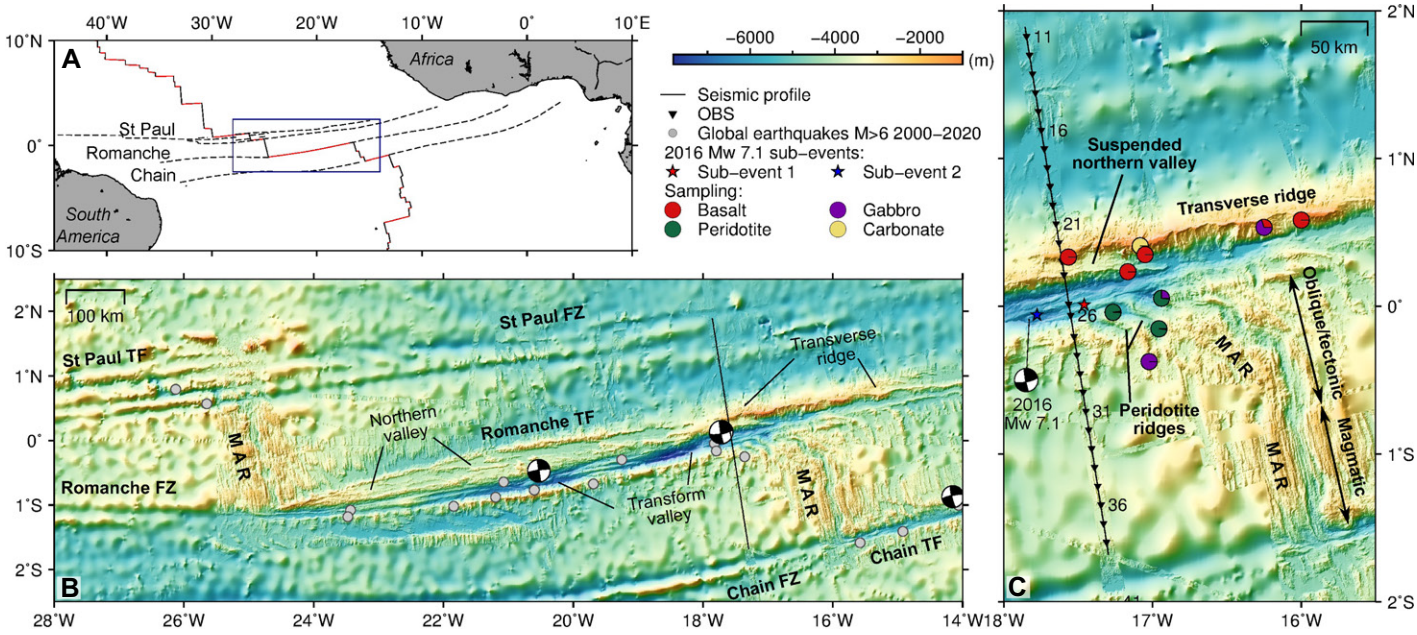

Figure 1. Study area. (A) Equatorial Mid-Atlantic Ridge, showing ridge axes (black solid), transform faults (red), and fracture zones (black dashed) of three large equatorial transforms. Outline of B is show by blue box. (B) Bathymetry of the Romanche transform fault (Bonatti et al., 1996), showing recent earthquakes of M >6 and focal mechanisms of M >7. (C) Close-up of the eastern Romanche ridge-transform intersection (RTI), showing the seismic experiment location, key sample locations (Bonatti et al., 1996), and the epicenter, focal mechanism, and modeled subevents of the 2016 Mw 7.1 earthquake (Hicks et al., 2020). TF—transform fault; FZ—fracture zone; MAR—Mid-Atlantic Ridge; OBS—ocean bottom seismograph.

Supplemental Material[1]), and their traveltimes were picked and inverted to obtain a two-dimensional P-wave velocity (Vp) model (Fig. 2).

We observe a clear change in the nature of the crust across the TF (Fig. 2; Fig. S3). To the north of the TF, a "normal" oceanic crustal velocity structure is apparent, with an average thickness of ~6 km and average velocity of 5–6 km/s in the upper crust down to 3 km below basement, and ~7 km/s in the lower crust (2 km above the Moho). We interpret this as "classic" mafic crustal structure, in agreement with the dredged basalt and gabbro samples (Bonatti and Honnorez, 1976), where the Moho represents a petrological (gabbro-peridotite) boundary. The normal velocity observed within the transverse ridge supports its formation through the transpression and uplift of a crustal section (Bonatti et al., 1994), similar to other Atlantic transverse ridges (Abrams et al., 1988; Marjanović et al., 2020). The lack of a significant velocity reduction beneath the suspended northern valley suggests that fracturing caused by the ancient TF has since been sealed (Roland et al., 2012). Conversely, to the south of the TF, the seismic crust displays highly variable thickness (3.5–6 km). Although the velocities just below the seafloor are low, indicating the presence of a thin layer of basalt or dolerite, the average velocities in the upper (~5.5–6.8 km/s) and lower crust (~7.5 km/s) are high (Fig. S3), suggestive of the presence of gabbro in the upper crust and serpentinized peridotite in the lower crust, particularly where Vp >7.5 km/s. This interpretation is consistent with the irregular seafloor topography, segmented and oblique ridge axis (Fig. 1C), and the presence of serpentinized peridotite (Bonatti et al., 2001), indicative of magma-poor crust, south of the TF.

Within the transform valley, we observe a 15–20-km-wide, low-velocity anomaly extending down to 9 km below the seafloor (bsf), with an amplitude of ~1 to 1.5 km/s in the upper crust, ~0.5 km/s in the lower crust, and up to 1 km/s in the upper mantle. The observation of PmP arrivals indicates the presence of a Moho and a crustal thickness of 5.5–6.5 km (Fig. 2; Figs. S3 and S4). Due to the ambiguity of seismic velocities, the seismically defined crust above the observed Moho can be interpreted as either fractured mafic rocks (Van Avendonk et al., 1998; Roland et al., 2012) or serpentinized peridotites beneath a thin basaltic layer (White et al., 1984). We next employ shipboard gravity data and effective medium analyses to further investigate the properties and composition of the lithosphere beneath the transform valley.

TRANSFORM VALLEY COMPOSITION

Comparison of residual gravity anomalies with a density model of homogeneous crust and mantle reveals an ~20 mGal negative gravity anomaly within the transform zone. Forward modeling shows that the inclusion of −200 kg/m^3 crustal and mantle density anomalies beneath the transform valley can fit the observed data (Fig. S5).

For our interpretation, we used a differential effective medium theory (Taylor and Singh, 2002) to quantify rock properties from the velocity and density anomalies (Fig. S9). Below the Moho, the velocity and density anomalies are consistent with an average of ~30% serpentinization, and up to ~50% serpentinization just below the Moho. Above the Moho, we consider two end-member models. Our modeling suggests that the anomalies in the crust can be explained by either (1) fractured mafic crust with an average porosity of up to ~10%, potentially ranging from ~1% at the Moho to ~15% at the seafloor (model 1, Fig. 3), or (2) fully serpentinized peridotite (100%) with little to no porosity, although at least ~5% porosity is needed to explain the low velocities at the seafloor (model 2, Fig. 3). Increasing the porosity would reduce the percentage of required serpentinization, but high levels of serpentinization (80%–100%) are consistent with recovered samples (Seyler and Bonatti, 1997).

Observations from the Gofar OTF in the Pacific Ocean suggest that weak zones along OTFs do not release stress by failing during large earthquakes but instead host small microearthquakes and swarms or slip aseismically (Froment et al., 2014). If the rocks above the Moho in the transform valley are dominantly

[1]Supplemental Material. Detailed methods and supplemental Figures S1–S9. Please visit https://doi.org/10.1130/GEOL.S.14582778 to access the supplemental material, and contact editing@geosociety.org with any questions.

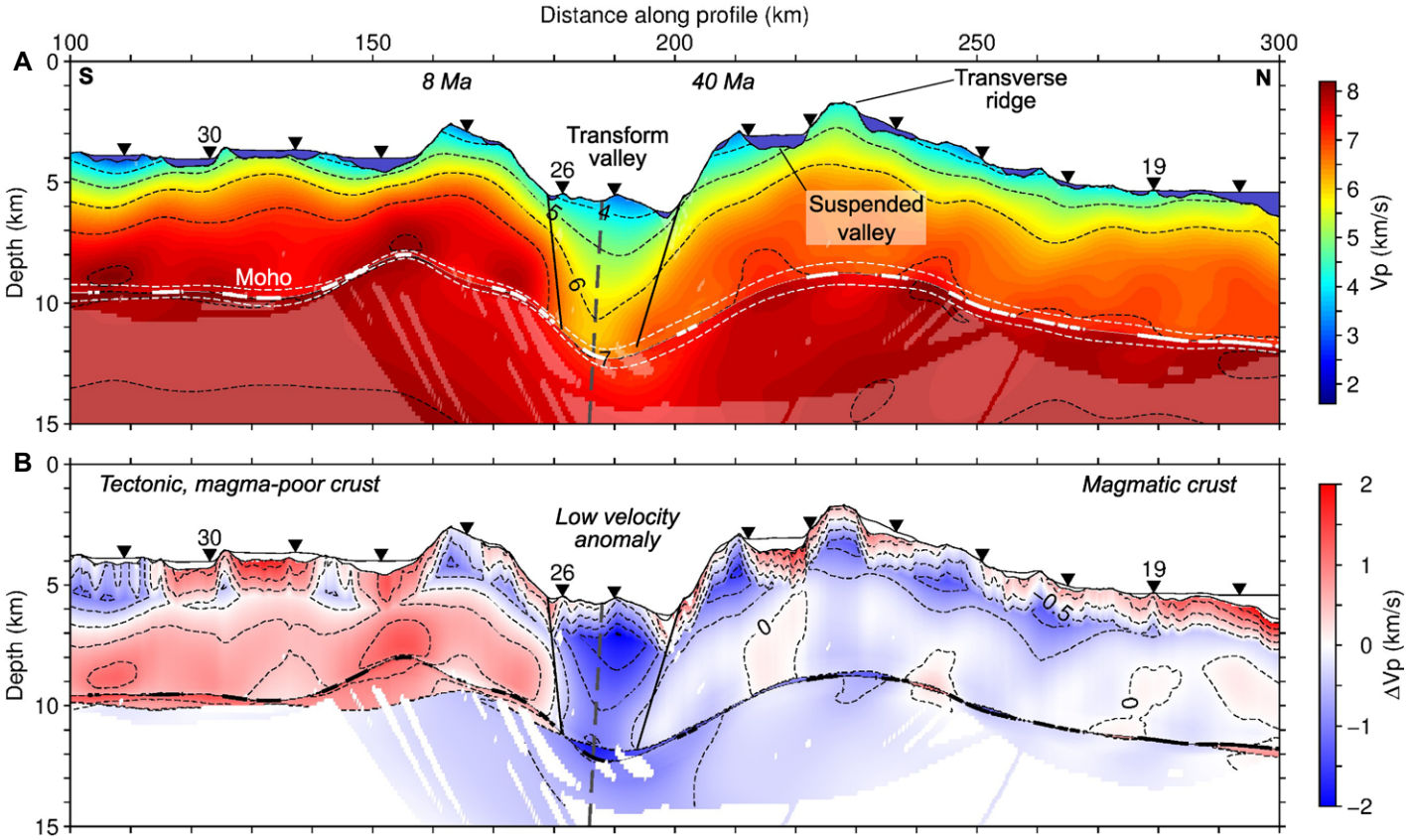

Figure 2. (A) Final averaged P-wave velocity model from tomographic inversion, and (B) velocity anomaly (final – initial), emphasizing low-velocity zone within transform valley. Gray dashed line shows fault plane located by Hicks et al. (2020), and black solid lines are interpreted valley-bounding faults. Ocean bottom seismographs (OBSs) are shown as black triangles, with those shown in Figure S1 (see footnote 1) labeled. Moho is shown in thin white, with its standard deviation in dashed white, and modeled Moho reflectors (PmP) are shown in thick white. Lighter colors show limits of ray coverage.

~80% serpentinized peridotite (Fig. 3B), this would have a significant weakening effect on the rheology of the segment (Escartín et al., 1997; Hirth and Guillot, 2013), and hence it is less likely to have hosted the large, crustal-depth rupture accompanying the 2016 Mw 7.1 earthquake (Hicks et al., 2020). The occurrence of larger (M >6) earthquakes on this segment of the fault (Fig. 1) suggests this is a stronger, more seismically coupled segment, in agreement with recent results from microseismicity (Yu et al., 2021). Mafic crust, consisting of lower-crustal gabbro

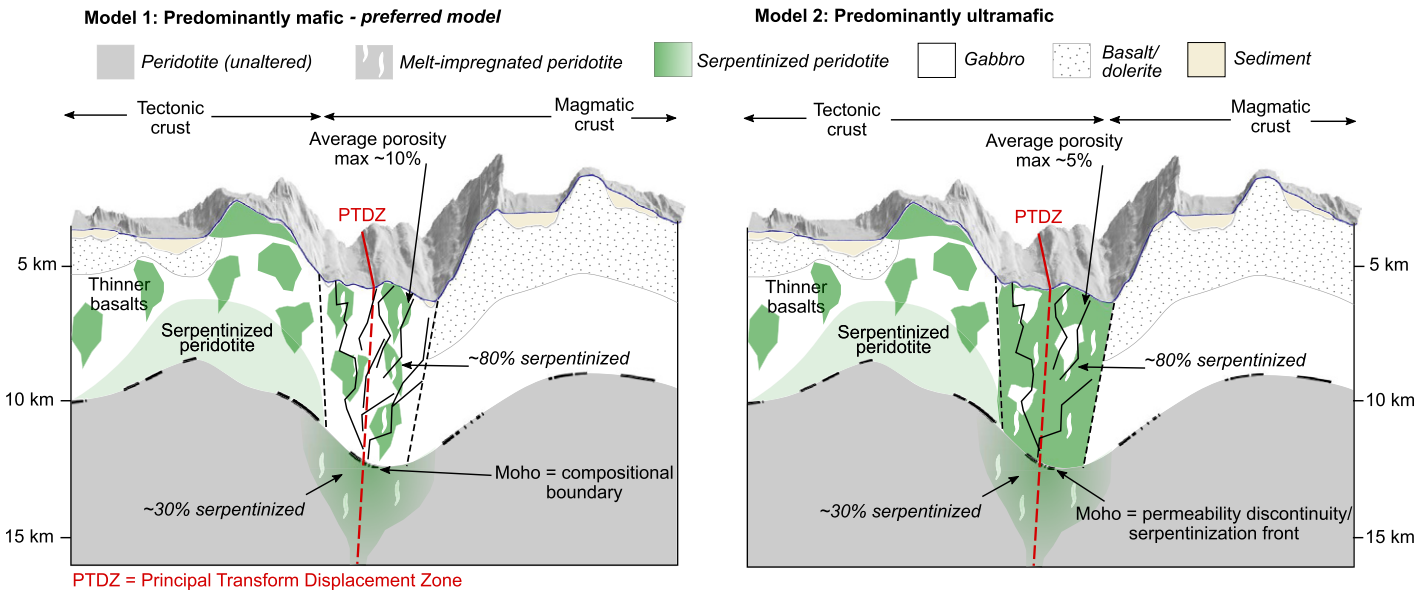

Figure 3. Two conceptual models of composition within transform zone beneath shaded relief bathymetry, consisting of either predominantly gabbroic material (model 1) or predominantly serpentinized peridotite (model 2). Thick black line shows PmP reflection points along Moho.

(model 1), would be strong and more capable of hosting large earthquakes.

In the case of model 1, the observed Moho boundary would represent a lithological change from gabbro to mantle serpentinized peridotite (Fig. 3A). However, in the case of model 2, the Moho would be caused by a relatively abrupt change in serpentinization from 80% above the Moho to ~50% below. As the serpentinization process tends to be gradual, such an abrupt change would likely require a preexisting permeability front. This is possible, but we did not find previous observations that support this possibility. Therefore, although both models remain plausible, our preferred model is that the thick seismic crust beneath the Romanche TF along our profile consists principally of mafic rocks.

DISCUSSION

Our observation of thick seismic crust beneath the Romanche OTF differs from the previous conceptions for long age-offset OTFs consisting of thinned or ultramafic "crust" (White et al., 1984; Detrick et al., 1993), such as that observed at the Charlie Gibbs (Whitmarsh and Calvert, 1986) and Oceanographer (Ambos and Hussong, 1986) OTFs. This result is surprising, because fertile mantle rocks and basalts recovered from the Romanche OTF and its adjacent MAR segments suggest low degrees of melting and cold mantle temperatures in the equatorial Atlantic (Schilling et al., 1994; Bonatti et al., 2001; Ligi et al., 2005). Our velocity model (Fig. 2A) south of the OTF is consistent with a reduction in magmatic material, with part of this region suggested to comprise <10% gabbro by Bonatti et al. (2001). However, our model also shows that the northern segment consists of thick, magmatic crust, and the transverse ridge, including the suspended northern valley, represents a thick section of magmatic material, confirmed by the sampling of basalts along its length (Fig. 1; Bonatti et al., 1994). These significant amounts of melt in the area could have formed a thick, mafic crust within the transform valley, with structure more similar to Pacific transforms such as Clipperton (Van Avendonk et al., 1998) and Gofar (Roland et al., 2012). It is likely that the mafic crust contains pockets of serpentinite, resulting from tectonism in the fault zone and extensive fluid flow along the fractures. Interestingly, at the 5°S Atlantic OTF, Planert et al. (2009) found >5-km-thick crust in one location along the transform valley, consistent with uniformly thick crust to the north. In contrast, elsewhere they found 3-km-thick crust, bounded by a segment that, though highly magmatic, displayed strong focusing of melt. These results suggest that the three-dimensional dynamics of magma distribution along the bounding segments—whether uniform, heterogeneous, or focused to the segment center—may control the composition of the transform valley and make it highly heterogeneous along strike.

The heterogeneity along OTFs will influence the dynamics of earthquake rupture, as has been observed at the Gofar TF (Roland et al., 2012; Froment et al., 2014), where fractured damage zones limit the propagation of large ruptures. Modeling of the 2016 Romanche earthquake (Hicks et al., 2020) revealed that it initiated in the mantle at 17 km depth, propagated to the east to a shallower depth (10 km), and then reversed direction and propagated at a supershear speed back to the west, rupturing principally the crustal rocks (Fig. 1). We suggest that the supershear ruptured section of this fault, sampled by our profile, more likely consists of gabbroic crust. The limit of rupture to the east coincides with two peridotite ridges (Yu et al., 2021), which could indicate a change in the composition to serpentinized peridotite. At the western limit, there lies a deep basin, which is likely to have a different lithology. Thus, the boundaries of the rupture could have been controlled, in this case, by the heterogeneity in crustal structure along the fault, with areas of serpentinized peridotite creating relatively weak barrier zones, while gabbroic crust acted as an asperity region. The distinct change in crustal structure and velocity across the TF may explain the westward direction of the supershear rupture (Hicks et al., 2020).

At both fast (Roland et al., 2012) and slow-slipping OTFs (Whitmarsh and Calvert, 1986; Ambos and Hussong, 1986), the observed low-velocity zones, and any serpentinization, are more often confined to the seismic crust, with the Moho representing a transition to unaltered mantle peridotite, although this may be due to poor sampling of the upper mantle. However, we have found extensive serpentinization of the upper mantle to at least 2.5 km below the Moho (>9 km sub-seafloor), indicating the potential for deep mantle hydration at OTFs, which may occur irrespective of slip rate (Van Avendonk et al., 2001). Hydrated OTF/FZ lithosphere would influence the dynamics of volcanism and seismicity along arcs, and earthquake processes at subduction zones (Cooper et al., 2020).

CONCLUSIONS

We have observed a thick, likely mafic, crust at the Romanche OTF, which can be considered to be an end member of slow-slipping transforms, as compared to thin or ultramafic crust as predicted at these plate boundaries. The crust north of the OTF appears to be mafic in composition, whereas that to the south is consistent with a more amagmatic origin. Slow-slipping OTFs are likely be highly heterogeneous along strike, with the structure dependent on local melt dynamics during formation, geometry of the fault, and any transtensional or transpressional stresses, and not solely on the thermal effect of old, cold lithosphere opposite the RTI.

ACKNOWLEDGMENTS

We thank the crew, technicians, and scientists aboard the N/O *Pourquoi Pas?* for their expertise during the ILAB-SPARC cruise. Thanks go to D. Brunelli and B. Debret for useful discussions on petrology and serpentinization, to L. Li for codes to calculate the mantle gravity thermal anomaly, and to K. Growe for contributions on traveltime picking and model building. Discussions with A. Schubnel on supershear ruptures were highly valuable. Constructive comments from T. Minshull and an anonymous reviewer helped to improve the paper. This project was funded by the European Research Council Advanced grant no. 339442 TransAtlanticILAB.

REFERENCES CITED

Abrams, L.J., Detrick, R.S., and Fox, P.J., 1988, Morphology and crustal structure of the Kane fracture zone transverse ridge: Journal of Geophysical Research, v. 93, B4, p. 3195–3210, https://doi.org/10.1029/JB093iB04p03195.

Ambos, E.L., and Hussong, D.M., 1986, Oceanographer transform fault structure compared to that of surrounding oceanic crust: Results from seismic refraction data analysis: Journal of Geodynamics, v. 5, p. 79–102, https://doi.org/10.1016/0264-3707(86)90024-4.

Bird, P., 2003, An updated digital model of plate boundaries: Geochemistry Geophysics Geosystems, v. 4, p. 1–52, https://doi.org/10.1029/2001GC000252.

Blackman, D.K., and Forsyth, D.W., 1989, Axial topographic relief associated with ridge-transform intersections: Earth and Planetary Science Letters, v. 95, p. 115–129, https://doi.org/10.1016/0012-821X(89)90171-4.

Bonatti, E., 1968, Ultramafic rocks from the Mid-Atlantic Ridge: Nature, v. 219, p. 363–364, https://doi.org/10.1038/219363a0.

Bonatti, E., and Honnorez, J., 1976, Sections of the Earth's crust in the equatorial Atlantic: Journal of Geophysical Research, v. 81, p. 4104–4116, https://doi.org/10.1029/JB081i023p04104.

Bonatti, E., Ligi, M., Gasperini, L., Peyve, A., Raznitsin, Y., and Chen, Y.J., 1994, Transform migration and vertical tectonics at the Romanche fracture zone, equatorial Atlantic: Journal of Geophysical Research: Solid Earth, v. 99, B11, p. 21779–21802, https://doi.org/10.1029/94JB01178.

Bonatti, E., Ligi, M., Carrara, G., Gasperini, L., Turko, N., Perfiliev, S., Peyve, A., and Sciuto, P.F., 1996, Diffuse impact of the Mid-Atlantic Ridge with the Romanche transform: An ultracold ridge-transform intersection: Journal of Geophysical Research: Solid Earth, v. 101, B4, p. 8043–8054, https://doi.org/10.1029/95JB02249.

Bonatti, E., Brunelli, D., Fabretti, P., Ligi, M., Asunta, R.P., and Seyler, M., 2001, Steady-state creation of crust-free lithosphere at cold spots in mid-ocean ridges: Geology, v. 29, p. 979–982, https://doi.org/10.1130/0091-7613(2001)029<0979:SSCOCF>2.0.CO;2.

Cannat, M., Mamaloukas-Frangoulis, V., Auzende, J.-M., Bideau, D., Bonatti, E., Honnorez, J., et al., 1991, A geological cross-section of the Vema fracture zone transverse ridge, Atlantic Ocean: Journal of Geodynamics, v. 13, p. 97–117, https://doi.org/10.1016/0264-3707(91)90034-C.

Cooper, G.F., Macpherson, C.G., Blundy, J.D., Maunder, B., Allen, R.W., Goes, S., et al., 2020, Variable water input controls evolution of the Lesser Antilles volcanic arc: Nature, v. 582, p. 525–529, https://doi.org/10.1038/s41586-020-2407-5.

DeMets, C., Gordon, R.G., and Argus, D.F., 2010, Geologically current plate motions: Geophysical Journal International, v. 181, p. 1–80, https://doi.org/10.1111/j.1365-246X.2009.04491.x.

Detrick, R.S., White, R.S., and Purdy, G.M., 1993, Crustal structure of North Atlantic fracture zones: Reviews of Geophysics, v. 31, p. 439–458, https://doi.org/10.1029/93RG01952.

Escartín, J., Hirth, G., and Evans, B., 1997, Effects of serpentinization on the lithospheric strength and the style of normal faulting at slow-spreading ridges: Earth and Planetary Science Letters, v. 151, p. 181–189, https://doi.org/10.1016/S0012-821X(97)81847-X.

Froment, B., McGuire, J.J., van der Hilst, R.D., Gouédard, P., Roland, E.C., Zhang, H., and Collins, J.A., 2014, Imaging along-strike variations in mechanical properties of the Gofar transform fault, East Pacific Rise: Journal of Geophysical Research: Solid Earth, v. 119, p. 7175–7194, https://doi.org/10.1002/2014JB011270.

Hensen, C., Duarte, J.C., Vannucchi, P., Mazzini, A., Lever, M.A., Terrinha, P., et al., 2019, Marine transform faults and fracture zones: A joint perspective integrating seismicity, fluid flow and life: Frontiers of Earth Science, v. 7, https://doi.org/10.3389/feart.2019.00039.

Hicks, S.P., Okuwaki, R., Steinberg, A., Rychert, C., Abercrombie, R., Bogiaztis, P., Schlaphorst, D., Zahradnik, J., Kendall, M., Yagi, Y., Shimizu, K., and Sudhaus, H., 2020, Back-propagating super-shear rupture in the 2016 M7.1 Romanche transform fault earthquake: Nature Geoscience, v. 13, p. 647–653, https://doi.org/10.1038/s41561-020-0619-9.

Hirth, G., and Guillot, S., 2013, Rheology and tectonic significance of serpentinite: Elements, v. 9, p. 107–113, https://doi.org/10.2113/gselements.9.2.107.

Hooft, E.E.E., Detrick, R.S., Toomey, D.R., Collins, J.A., and Lin, J., 2000, Crustal thickness and structure along three contrasting spreading segments of the Mid-Atlantic Ridge, 33.5°–35°N: Journal of Geophysical Research: Solid Earth, v. 105, B4, p. 8205–8226, https://doi.org/10.1029/1999JB900442.

Ligi, M., Bonatti, E., Gasperini, L., and Poliakov, A.N.B., 2002, Oceanic broad multifault transform plate boundaries: Geology, v. 30, p. 11–14, https://doi.org/10.1130/0091-7613(2002)030<0011:OBMTPB>2.0.CO;2.

Ligi, M., Bonatti, E., Cipriani, A., and Ottolini, L., 2005, Water-rich basalts at mid-ocean-ridge cold spots: Nature, v. 434, p. 66–69, https://doi.org/10.1038/nature03264.

Maia, M., Sichel, S., Briais, A., Brunelli, D., Ligi, M., Ferreira, N., et al., 2016, Extreme mantle uplift and exhumation along a transpressive transform fault: Nature Geoscience, v. 9, p. 619–623, https://doi.org/10.1038/ngeo2759.

Marjanović, M., Singh, S.C., Gregory, E.P.M., Grevemeyer, I., Growe, K., Vaddineni, V., Laurencin, M., Carton, H., Gómez de la Peña, L., and Filbrandt, C., 2020, Seismic crustal structure and morphotectonic features associated with the Chain fracture zone and their role in the evolution of the Equatorial Atlantic region: Journal of Geophysical Research: Solid Earth, v. 125, p. e2020JB020275, https://doi.org/10.1029/2020JB020275.

McGuire, J.J., Ihmlé, P.F., and Jordan, T.H., 1996, Time-domain observations of a slow precursor to the 1994 Romanche transform earthquake: Science, v. 274, p. 82–85, https://doi.org/10.1126/science.274.5284.82.

Planert, L., Flueh, E., and Reston, T., 2009, Along- and across-axis variations in crustal thickness and structure at the Mid-Atlantic Ridge at 5°S obtained from wide-angle seismic tomography: Implications for ridge segmentation: Journal of Geophysical Research: Solid Earth, v. 114, B09102, https://doi.org/10.1029/2008JB006103.

Prinz, M., Keil, K., Green, J.A., Reid, A.M., Bonatti, E., and Honnorez, J., 1976, Ultramafic and mafic dredge samples from the Equatorial Mid-Atlantic Ridge and fracture zones: Journal of Geophysical Research, v. 81, p. 4087–4103, https://doi.org/10.1029/JB081i023p04087.

Roland, E., Lizarralde, D., McGuire, J.J., and Collins, J.A., 2012, Seismic velocity constraints on the material properties that control earthquake behavior at the Quebrada-Discovery-Gofar transform faults, East Pacific Rise: Journal of Geophysical Research: Solid Earth, v. 117, B11102, https://doi.org/10.1029/2012JB009422.

Schilling, J.-G., Hanan, B.B., McCully, B., Kingsley, R.H., and Fontignie, D., 1994, Influence of the Sierra Leone mantle plume on the equatorial Mid-Atlantic Ridge: A Nd-Sr-Pb isotopic study: Journal of Geophysical Research: Solid Earth, v. 99, B6, p. 12005–12028, https://doi.org/10.1029/94JB00337.

Seyler, M., and Bonatti, E., 1997, Regional-scale melt-rock interaction in lherzolitic mantle in the Romanche fracture zone (Atlantic Ocean): Earth and Planetary Science Letters, v. 146, p. 273–287, https://doi.org/10.1016/S0012-821X(96)00220-8.

Taylor, M.A.J., and Singh, S.C., 2002, Composition and microstructure of magma bodies from effective medium theory: Geophysical Journal International, v. 149, p. 15–21, https://doi.org/10.1046/j.1365-246X.2002.01577.x.

Van Avendonk, H.J.A., Harding, A.J., Orcutt, J.A., and McClain, J.S., 1998, A two-dimensional tomographic study of the Clipperton transform fault: Journal of Geophysical Research: Solid Earth, v. 103, B8, p. 17885–17899, https://doi.org/10.1029/98JB00904.

Van Avendonk, H.J.A., Harding, A.J., Orcutt, J.A., and McClain, J.S., 2001, Contrast in crustal structure across the Clipperton transform fault from travel time tomography: Journal of Geophysical Research: Solid Earth, v. 106, B6, p. 10961–10981, https://doi.org/10.1029/2000JB900459.

White, R., Detrick, R., Sinha, M., and Cormier, M., 1984, Anomalous seismic crustal structure of oceanic fracture zones: Geophysical Journal International, v. 79, p. 779–798, https://doi.org/10.1111/j.1365-246X.1984.tb02868.x.

Whitmarsh, R.B., and Calvert, A.J., 1986, Crustal structure of Atlantic fracture zones—I. The Charlie-Gibbs fracture zone: Geophysical Journal of the Royal Astronomical Society, v. 85, p. 107–138, https://doi.org/10.1111/j.1365-246X.1986.tb05174.x.

Yu, Z., Singh, S.C., Gregory, E.P.M., Maia, M., Wang, Z., and Brunelli, D., 2021, Semi-brittle seismic deformation in high-temperature mantle mylonite shear zone along the Romanche transform fault: Science Advances, v. 7, p. eabf3388 , https://doi.org/10.1126/sciadv.abf3388.

Printed in USA